engineering fracture mechanics

an international journal

EDITOR-IN-CHIEF
H. LIEBOWITZ

COMBINED NONLINEAR AND LINEAR (MICRO AND MACRO) FRACTURE MECHANICS APPLICATIONS TO MODERN ENGINEERING STRUCTURES

PERGAMON PRESS
New York · Oxford · Braunschweig

Engineering Fracture Mechanics

Volume 7 Number 3 September 1975

CONTENTS

ISBN 0 08 019982 8

Printed in Great Britain by A. Wheaton & Co., Exeter

Engineering Fracture Mechanics, 1975, Vol. 7, pp. 367–369. Pergamon Press. Printed in Great Britain

FOREWORD

SELECTED papers appearing in this issue of the Journal of Engineering Fracture Mechanics were presented at the U.S.–Japan Seminar under the direction of Professor T. Yokobori and Professor H. Liebowitz. This seminar concerned itself with the combined nonlinear and linear (micro and macro) fracture mechanics applications to modern engineering structures. The Japan Society for the Promotion of Science and the U.S. National Science Foundation sponsored this meeting under the bilateral agreement between both countries. This meeting was held in Sendai, Japan during the period of 12–16 August 1974. Participants and observers invited were:

Participants

H. Liebowitz	Professor (U.S. Organizer)	Dean, School of Engineering and Applied Science, George Washington University, U.S.A.
T. Yokobori	Professor (Japanese Organizer)	Department of Mechanical Engineering II and Director, The Research Institute for Strength and Fracture of Materials, Tohoku University, Japan.
J. M. Barsom	Asst. Research Consultant	Research Laboratory, U.S. Steel Corporation, U.S.A.
F. R. Eirich	Professor	Polytechnic Institute of New York, U.S.A.
T. H. Erismann	President	EMPA, Switzerland
G. T. Hahn	Section Manager	Metal Science Division, Battelle Memorial Institute, U.S.A.
M. Ichikawa	Asst. Professor	The Research Institute for Strength and Fracture of Materials, Tohoku University Japan
A. Kamei	Asst. Professor	Department of Mechanical Engineering II, Tohoku University, Japan
T. Kanazawa	Professor	Department of Naval Architecture, University of Tokyo, Japan
T. Kawasaki	Professor	Department of Mechanical Engineering II, Tohoku University, Japan
H. Kitagawa	Professor	Institute of Industrial Science, University of Tokyo, Japan
H. Nakamura	Honorary Director	Research Institute, Ishikawajima-Harima Heavy Industries Co., Ltd., Japan
H. Nishitani	Professor	Faculty of Engineering, Kyushu University, Japan
K. Ohji	Professor	Department of Mechanical Engineering, Osaka University, Japan
H. Okamura	Professor	Department of Mechanical Engineering, University of Tokyo, Japan
A. Otsuka	Professor	Department of Iron and Steel Engineering, Nagoya University, Japan

E. R. Parker	Professor	Department of Materials Science and Engineering, University of California, U.S.A.
Yu. N. Rabotnov	Professor	Department of Mechanics and Mathematics, Moscow University, U.S.S.R.
G. C. Sih	Professor	Institute of Fracture and Solid Mechanics, Lehigh University, U.S.A.
S. Tanaka	Professor	Department of Mechanical Engineering, University of Electro-communications, Japan
R. E. Zinkham	Director	Mechanical Metallurgy Division, Reynolds Metals Co., U.S.A.

Observers

M. Arii	Manager	Heavy Apparatus Engineering Laboratory, Tokyo Shibaura Electric Co., Ltd., Japan
C. J. Astill	Asst. Program Director	Mechanics Section, Division of Engineering Research, National Science Foundation, U.S.A.
S. C. Chou	Research Engineer	A.M. & M. Research Center, U.S.A.
B. Cummings	Professor	A.B. Research Labs. & Adjunct Professor, Johns Hopkins University, U.S.A.
K. Ikeda	Director	Structural Engineering Laboratory, Kobe Steel Ltd., Japan
M. Ishida	Professor	Faculty of Engineering, Kyushu University, Japan
K. Ishikawa	Chief	Yokohama No. 3. Works, Ishikawajima–Harima Heavy Industries Co., Ltd., Japan
D. Jones	Assoc. Professor	School of Engineering and Applied Science, George Washington University, U.S.A.
M. Kawahara	Manager	Technical Research Center, Nippon Kokan K. K., Japan
S. Konosu	Graduate	Department of Mechanical Engineering II, Tohoku University, Japan
T. Kunio	Professor	Department of Mechanical Engineering, Keio University, Japan
A. Nagai	Chief Researcher	Technical Research Institute, Hitachi Shipbuilding and Engineering Co., Ltd., Japan
M. Nagao	Researcher	Hitachi Research Laboratory, Hitachi Ltd., Japan
M. Nagumo	Manager	Fundamental Research Laboratories, Nippon Steel Corporation, Japan
Y. Sawaki	Asst. Professor	Department of Mechanical Engineering II, Tohoku University, Japan
J. Wantanabe	General Manager	Research Laboratory, Muroran Plant, The Japan Steel Works, Ltd., Japan
R. J. Wolfe	Head	Materials Department, Naval Ship Research & Development Center, U.S.A.

H. A. Wood	Technical Manager	A.F. Flight Dynamics Labs., Wright–Patterson A.F.B., U.S.A.
H. Yajima	Senior Research Engineer	Nagasaki Technical Institute, Mitsubishi Heavy Industries, Ltd., Japan
H. Yamanouchi	Manager	Nagasaki Technical Institute, Mitsubishi Heavy Industries, Ltd., Japan
A. T. Yokobori, Jr.	Graduate	Department of Mechanical Engineering II, Tohoku University, Japan

The papers chiefly addressed themselves to: (1) principal facets of the nonlinear fracture mechanics theories, (2) results and possibilities of combined Microscopic and Macroscopic viewpoints of fracture mechanics, and (3) problems of applying these combined research results, in a unified manner if possible, to modern engineering structure.

The current status regarding fracture mechanics is one in which linear elastic fracture mechanics (LEFM) has become widely accepted as defining certain fundamental properties of high-strength materials. Many industries which employ such materials in structural applications now routinely require certain fracture mechanics criteria, such as plane strain fracture toughness, as part of the materials selection and design procedures. However, the principal limitation of LEFM is its intrinsic restriction to situations of small crack-tip plastic deformation prior to fracture. Thus, a considerable amount of research has been conducted in recent years with the objective of incorporating significant amounts of inelastic crack-tip behavior into fracture mechanics results.

Most research efforts at broadening the range of applicability of fracture mechanics to include significant nonelastic behavior have followed along two key directions. The thrust of one of these research efforts has been to include, from a macroscopic viewpoint, crack-tip plasticity and slow crack growth into a nonlinear theory of fracture mechanics. The second approach has involved the correlation of combined microscopic and macroscopic fracture mechanics considerations within the general context of LEFM. The U.S.–Japan Cooperative Science Program International Seminar emphasized as indicated above, combined the microscopic and macroscopic viewpoints, and nonlinear work, along with fracture mechanics applications to modern engineering structures. Much of the success achieved at this seminar was due mainly to the participants and observers of the seminar. Special acknowledgement should be given to the Japan Society for the Promotion of Science and the National Science Foundation for making this seminar possible.

T. YOKOBORI

H. LIEBOWITZ

Engineering Fracture Mechanics, 1975, Vol. 7, pp. 371–375. Pergamon Press. Printed in Great Britain

MICROSTRUCTURAL FEATURES AFFECTING FRACTURE TOUGHNESS OF HIGH STRENGTH STEELS

EARL R. PARKER and VICTOR F. ZACKAY
Department of Materials Science and Engineering, University of California, Berkeley, CA 94721, U.S.A.

Abstract—The fracture toughness of quenched and tempered steels, such as AISI 4340, AISI 4130 and 300M, can be increased by 50–100% by minor changes in heat treating procedures. Certain microstructural features, particularly blocky ferrite, upper bainite and twinned martensite plates, are deleterious to fracture toughness. Similarly, the presence of undissolved carbides and sulfide inclusions, which act as crack nuclei, can lower fracture toughness by 25–50%. Other microstructural constituents, such as lower bainite, autotempered martensite, and retained austenite can enhance fracture toughness. By controlling the amounts and distributions of the microstructural constituents, the fracture toughness values of AISI 4340, AISI 4130 and 300M can be raised to the fracture toughness level of 18Ni maraging steel at equivalent values of yield strength.

INTRODUCTION

ULTRA-HIGH strength steels, such as AISI 4340 heat treated to have a yield strength over 200,000 psi, are relatively brittle when cracklike defects are present. An extensive research program has been underway in the author's laboratory during the past several years, with the objective of identifying the elements of defect structure and microstructure that have major effects upon the plane strain fracture toughness. Some elements of structure enhance fracture toughness, while others degrade this important property. The highlights of the various investigations involved are reported herein.

By minimizing or eliminating those microconstituents that lowered fracture toughness, and increasing those that enhanced it, the fracture toughness could be increased 50–100% above the values obtained with commercially used heat treatments. The optimization of properties could be attained by either of two means—(1) changing the heat treating procedure, or (2) changing the chemical composition of the alloy.

EXPERIMENTAL PROGRAM

In the heat treatment of steel, austenitizing is a critical step. In general, use of low austenitizing temperatures is preferred because this procedure produces the smallest austenite grain size—and presumably the best combination of mechanical properties. In the present investigation, it was quickly found that low austenitizing temperatures did not provide the maximum fracture toughness (measured in accordance with ASTM standard procedures). In fact, the reverse was found to be true, with increases of 50% or more being obtained when high austenitizing temperatures were used. (However, as is well known, slightly better elongation and reduction in area are obtained in tensile test bars that have been subjected to low austenitizing temperatures). The compositions of the steels used in the present investigation are listed in Table 1.

Table 1. Chemical compositions of steels

Designation	Compositions, Wt%								
	C	Cr	Mn	Mo	Ni	P	S	Si	V
0.30C-5Mo	0.30	-	0.60	5.03	-	0.008	0.005	<0.02	-
0.41C-5Mo	0.41	-	0.51	4.93	-	0.007	0.005	<0.02	-
0.34C-1Mo	0.34	-	0.63	0.95	-	0.008	0.005	<0.02	-
0.35C-1Mo-3Ni	0.35	-	0.61	0.95	3.1	0.007	0.005	<0.02	-
AISI 4130-A	0.31	0.85	0.57	0.18	0.15	0.008	0.009	0.28	<0.005
AISI 4130-B	0.33	0.90	0.63	0.18	0.15	0.008	0.009	0.27	<0.005
AISI 4330	0.28	0.85	1.02	0.40	1.80	0.009	0.005	0.28	0.07
AISI 4340	0.40	0.72	0.85	0.24	1.73	0.004	0.010	0.22	<0.005

One of the important factors influenced by austenitizing temperature is the presence of undissolved carbides in the microstructure. This was clearly shown by the work of Tom[1], who used special steels containing 0·30C–5Mo and 0·41C–5Mo in his investigation. Both strength and fracture toughness were found to increase with increasing austenitizing temperature, as shown in Fig. 1. Metallographic examinations revealed that undissolved carbides were present below about 1050°C in the 0·30C–5Mo steel, but not above this temperature. The plane strain fracture toughness of the steel increased suddenly from 50 ksi-in$^{1/2}$ to 100 ksi-in$^{1/2}$ when the austenitizing temperature was raised from 1000° to 1100°C. A similar, but more gradual, change was found for the 0·41C–5Mo steel. Experiments were made with several other steels of lower alloy content (e.g. 0·34C–1Mo and 0·35C–1Mo–3Ni). In these steels, all carbides were dissolved at 870°C and the fracture toughness values were found to be nearly independent of the austenitizing temperature (or grain size). These results are shown in Fig. 2.

Another important influence of austenitizing temperature is its effect on hardenability. Two factors affecting hardenability are the austenite grain size and the amount of carbon in solution. In steels of high hardenability, and in which all of the carbides are dissolved at low austenitizing temperatures, the grain size effect is not normally evident. This is so because the hardenability, even with the smaller grain size, is adequate to prevent the formation of ferrite and upper bainite during quenching. Low values of fracture toughness are generally associated with the presence of these transformation products. However, with steels of intermediate hardenability, such as AISI 4130, the effect of grain size (i.e. austenitizing temperature) may be very important[2]. In the present study when AISI 4130 steel was austenitized at 1200°C and ice-brine quenched, the fracture toughness was nearly twice as high as it was for the same steel oil quenched from 870°C. Oil quenching from 1200°C improved the fracture toughness relative to the lower temperature treatment, but less so than the more severe quench. The results are shown in Fig. 3. The tensile mechanical properties of as-quenched AISI 4130, AISI 4330 and AISI 4340 steels of the present investigation are listed in Table 2. The microstructural features of AISI 4130 steel differed for the various treatments, with the 870°C oil quench producing a mixture of blocky ferrite and martensite that was partially autotempered. The microstructure of the 1200°C ice-brine quenched material had no blocky ferrite; it consisted entirely of martensite (partially autotempered). A similar correspondence between heat treatment, fracture toughness, and microstructure existed

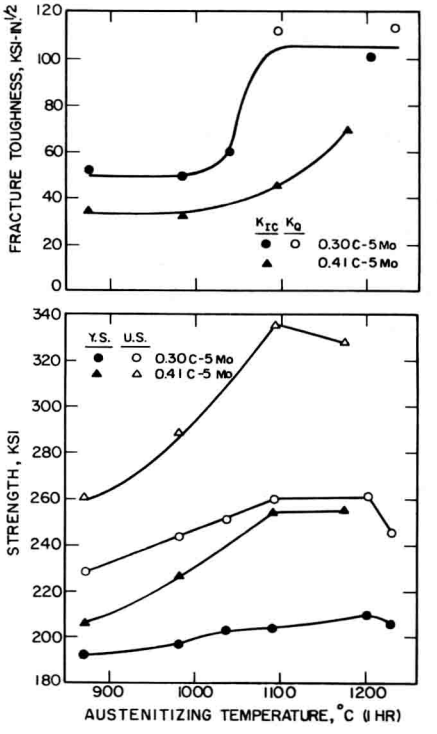

Fig. 1. Plots showing the influence of austenitizing temperature on room temperature fracture toughness (K_{IC} or K_Q), yield strength (Y.S.), and ultimate strength (U.S.) of 0·30C-5Mo and 0·41C-5Mo Steels.

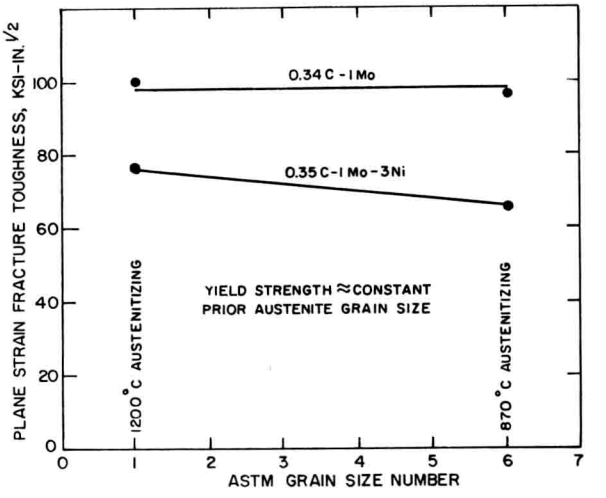

Fig. 2. Plots of room temperature plane strain fracture toughness vs prior austenite grain size (indicated by ASTM grain size number) for as-quenched 0·34C–1Mo and 0·35C–1Mo–3Ni steels.

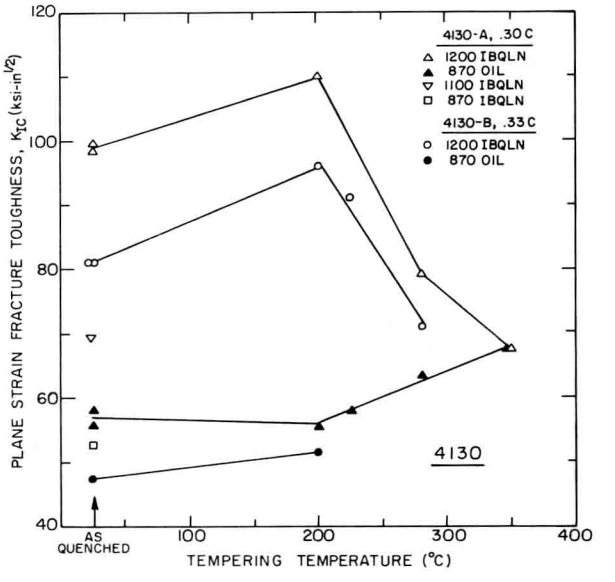

Fig. 3. Plots of room temperature plane strain fracture toughness vs tempering temperature for AISI 4130 steel. Austenitizing temperatures and quenching media are indicated. (IBQLN is an abbreviation for ice-brine quenching followed by refrigeration in liquid nitrogen).

for AISI 4330 steel. Plots of room temperature plane strain fracture toughness vs tempering temperature for two austenitizing treatments are shown in Fig. 4.

The use of high austenitizing treatments for steels having high hardenabilities, such as AISI 4340, also resulted in substantially higher K_{IC} values, even though there were no undissolved carbides, blocky ferrite, or upper bainite present in the microstructure resulting from the use of lower (870°C) quenching temperature. The room temperature fracture toughness of AISI 4340 steel is shown in Fig. 5 as a function of tempering temperature for two austenitizing temperatures. The preferred heat treatment involves a step-quench, i.e. cooling slowly from 1200° to 870°C before oil quenching. Quenching directly into oil from 1200°C tended to cause cracking, as did ice-brine quenching from 870°C. Step-quenching (1200°→870°C *OQ*) nearly doubled the as-quenched (870°C *OQ*) fracture toughness.

Optical metallographic examination failed to reveal any significant microstructural difference resulting from the two austenitizing treatments (other than differences in austenite grain size). Transmission electron microscopy was employed to reveal additional small-scale structural differences. It was found that the 1200°C material had a significant amount of retained austenite in the form of 100–200 Å thick films between martensite laths, whereas the 870°C material had very

Table 2. Tensile properties of As-quenched AISI 4130, AISI 4330 and AISI 4340 steels

Steel	Austenitizing Temp. (°C) and Quenching Medium	0.2% Offset Yield Strength, ksi	Ultimate Tensile Strength, ksi	Elong. %	Red. in Area %
AISI 4130	870, Oil	201	284	11.4	32.9
	1200, Oil	205	276	5.6	9.9
	1200, Ice-brine	215	249	1.6	6.6
AISI 4330	870, Oil	234	284	13.1	43
	1200, Ice-brine	210	222	0.6	3.4
AISI 4340	870, Oil	231	322	9.0	30.8
	1200+870, Oil	231	318	3.2	7.8

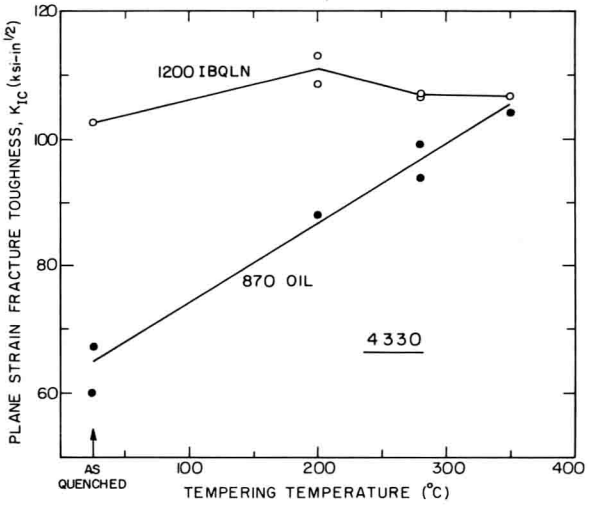

Fig. 4. Plots of room temperature plane strain fracture toughness vs tempering temperature for AISI 4330 steel. Austenitizing temperatures and quenching media are indicated.

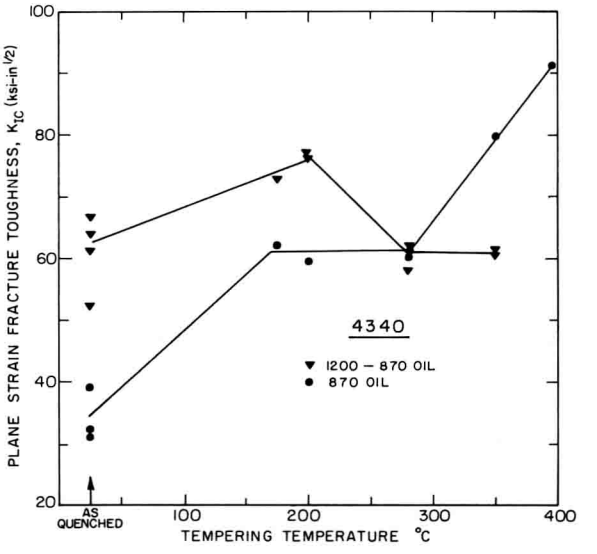

Fig. 5. Plots of room temperature plane strain fracture toughness vs tempering temperature for AISI 4340 steel. Austenitizing temperatures and quenching media are indicated.

few austenite films[5], as shown in Fig. 6. Austenite is tough and crack resistant. The beneficial effect of the higher temperature treatment was therefore attributed mainly to the presence of the austenite films. However, there was another distinct microstructural difference observed in the transmission electron microscope studies. The packets of lath martensite were similar for both austenitizing treatments, but the material heat treated at 870°C also had twinned martensite

plates. Das and Thomas[3] and Thomas[4] have shown that the presence of twinned martensite plates causes the fracture toughness to be lower than with lath martensite alone. This additional difference in microstructure is believed to have been partially responsible for the higher fracture toughness of the step-quenched steel.

Additional investigations of the effects of heat treatments and variations in chemical composition are continuing. Preliminary results indicate that even greater improvements in fracture toughness may be forthcoming.

Acknowledgements—The authors are grateful to Dr. Michael Yokota, Dr. George Lai, Dr. William Wood, Dr. Thomas Tom and Mr. Naga Prakash Babu for use of unpublished data, and Dr. M. Dilip Bhandarkar for many helpful discussions and critical technical review.

This work was performed partially under the auspices of the United States Atomic Energy Commission through the Lawrence Berkeley Laboratory, Inorganic Materials Research Division, and partially under the auspices of the Army Mechanics and Materials Research Center, Watertown, Mass., U.S.A.

REFERENCES

[1] T. Tom, Microstructural variables and fracture toughness of high strength Mo and Mo–Ni steels. D. Eng. Thesis, LBL-1856, University of California, Berkeley, Calif. (1973).
[2] W. E. Wood, E. R. Parker and V. F. Zackay, An investigation of metallurgical factors which affect the fracture toughness of ultra-high strength steels, LBL-1474, Lawrence Berkeley Laboratory, Berkeley, Calif., May (1973).
[3] S. K. Das and G. Thomas, Structure and mechanical properties of Fe–Ni–Co–C steels, *Trans. ASM* **62**, 659, (1969).
[4] G. Thomas, Electron microscopy investigations of ferrous martensite. *Met. Trans.* **2**, 2373, (1971).
[5] G. Y. Lai, W. E. Wood, R. A. Clark, V. F. Zackay and E. R. Parker, Effect of austenitizing temperature on the amount of retained austenite in AISI 4340 steel, *Met Trans.* (To be submitted) (1974).

Engineering Fracture Mechanics, 1975, Vol. 7, pp. 377–388. Pergamon Press. Printed in Great Britain

NON-LINEAR INTERACTION BETWEEN MAIN CRACK AND NEAR-BY SLIP BAND

T. YOKOBORI, M. YOSHIDA, H. KURODA, A. KAMEI and S. KONOSU
Department of Mechanical Engineering II, Tohoku University, Sendai, Japan

Abstract—Based on micro- and macro fracture mechanics, the basic equations for the general configuration of a crack (or a notch) and a slip band are obtained. As a special case, the coefficients of mutual interaction in stress intensity factors are calculated for the critical configuration of them corresponding to the low stress brittle fracture.

The coefficients of mutual interaction are given in terms of a simple and analytical formula with a sufficiently good approximation. Furthermore, both the stress intensity factors at the tip of the crack and at the end of the slip band are obtained in simple forms applicable to fracture problems.

1. INTRODUCTION

THE CONVENTIONAL fracture mechanics has developed from the study of homogeneous continuum mechanics that primarily deal with crack-type defects from the macroscopic standpoint. On the other hand, in physics of matter, the theories are mainly composed of the analysis of dislocations as the microscopic (lattice) defects. Real materials, however, contain inevitably defects of both types. From this point of view, the mechanical treatment for the strength and fracture of solids taking into account stress concentrations due to crack-type defect (macro-stress concentration) and due to dislocation-type defect (micro-stress concentration); namely, a concept of combined micro- and macro-fracture mechanics, has been proposed by one of the authors[1–4]. Also the stress intensity factors for the case when the distance between a crack tip and a slip band tip is fairly long has been obtained[5, 6]. For the case when this distance is short, the model that the near-by slip band is situated on the extension surface of the crack has been analysed and the coefficients of mutual interaction for the model have been calculated[7] and the physical meaning of the coefficients of mutual interaction have been clarified[7].

In the present paper, the basic equations for the general configuration of the crack and near-by slip band are derived by using the method of continuous distribution of infinitesimal dislocations. As a special case, the equations are solved for the critical configuration of a crack and a near-by slip band corresponding to low stress brittle fracture, and the coefficients of mutual interaction in stress intensity factors are calculated. Consequently, the mutual interaction coefficients are expressed in a simple and analytical formula with a sufficiently good approximation, which is valid for the case of the very short distance between crack tip and slip band tip. From the results, the stress intensity factors at the tip of the crack and at the end of the slip band are obtained in a simple form containing microscopic factors, that is, slip band length (= grain diameter) and frictional stress against dislocation movement, as well as macroscopic factors, that is, crack (or notch) length and applied stresses system, which are applicable to fracture problems.

2. THEORETICAL ANALYSIS

2.1 *The case of general configuration*

Let us consider an infinite elastic solid with a crack of length $2c$. The tensile stress σ is applied in the direction of angle Ψ inclined against the crack plane and the shear stress τ is applied in the direction perpendicular to σ at infinity as shown in Fig. 1. Suppose that under the action of σ and τ, a slip band of length $2d$ occurs in the region near the crack tip. Let θ, ω be the angles between the extension of the crack plane and the slip plane, and between the former and the plane $\overline{BP}$, respectively. And h represents a distance between the crack tip (B) and the slip band tip (P). For convenience, let $(O_1 - x_1, y_1)$ and $(O_2 - x_2, y_2)$ be two orthogonal coordinate systems introduced at the center of the crack and the slip band respectively, with the extension of the crack plane along x_1 axis and that of the slip plane along x_2 axis as shown in Fig. 1. The crack can be simulated by superposing two distributions of infinitesimal dislocations[8], $f_1(x_1)$ and $f_2(x_1)$, which are shown respectively in Figs. 2(a) and (b). The slip band can be simulated similarly by infinitesimal

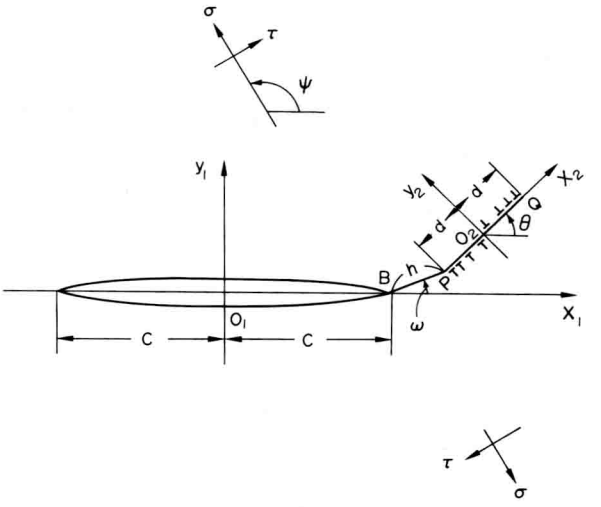

Fig. 1. An interaction model of a crack and a near-by slip band.

dislocations [8] $f_3(x_2)$ as shown in Fig. 2(c). From requirements of equilibrium of each dislocation, $f_1(x_1)$, $f_2(x_1)(-c < x_1 < c)$ and $f_3(x_2)(-d < x_2 < d)$ must satisfy the following equations:

$$\left.\begin{aligned}
&\sigma_{y_1} - A\int_{-c}^{c} \frac{f_1(\zeta_1)}{\zeta_1 - x_1}\,d\zeta_1 + A\int_{-d}^{d} K_1(x_1, \zeta_2) f_3(\zeta_2)\,d\zeta_2 = 0,\\
&\tau_{x_1 y_1} - A\int_{-c}^{c} \frac{f_2(\zeta_1)}{\zeta_1 - x_1}\,d\zeta_1 + A\int_{-d}^{d} K_2(x_1, \zeta_2) f_3(\zeta_2)\,d\zeta_2 = 0,\\
&\tau_m - \tau_i - A\int_{-d}^{d} \frac{f_3(\zeta_2)}{\zeta_2 - x_2}\,d\zeta_2 + A\int_{-c}^{c} K_3(x_2, \zeta_1) f_1(\zeta_1)\,d\zeta_1\\
&\qquad + A\int_{-c}^{c} K_4(x_2, \zeta_1) f_2(\zeta_1)\,d\zeta_1 = 0,
\end{aligned}\right\} \tag{1}$$

where

$A = Gb/[2\pi(1-\nu)]$,
G = Shear modulus,
ν = Poisson's ratio,
b = Burgers vector of a unit dislocation,

$$\left.\begin{aligned}
K_1(x_1, \zeta_2) &= \frac{-Y_1(Y_1^2 + X_1^2) + 2Y_1X_1^2\cos 2\theta + X_1(X_1^2 - Y_1^2)\sin 2\theta}{(X_1^2 + Y_1^2)^2},\\
K_2(x_1, \zeta_2) &= \frac{-2Y_1X_1^2\sin 2\theta + X_1(X_1^2 - Y_1^2)\cos 2\theta}{(X_1^2 + Y_1^2)^2},\\
K_3(x_2, \zeta_1) &= \frac{-2Y_2X_2^2\sin 2\theta - X_2(X_2^2 - Y_2^2)\cos 2\theta}{(X_2^2 + Y_2^2)^2},\\
K_4(x_2, \zeta_1) &= \frac{2Y_3X_3^2\sin 2\theta + X_3(X_3^2 - Y_3^2)\cos 2\theta}{(X_3^2 + Y_3^2)^2},\\
X_1 &= -(c - x_1)\cos\theta - h\cos(\theta - \omega) - (d + \zeta_2),\\
Y_1 &= (c - x_1)\sin\theta + h\sin(\theta - \omega),\\
X_2 &= h\sin\omega + (d + x_2)\sin\theta,\\
Y_2 &= -(c - \zeta_1) - h\cos\omega - (d + x_2)\cos\theta,\\
X_3 &= -Y_2,\\
Y_3 &= X_2.
\end{aligned}\right\} \tag{2}$$

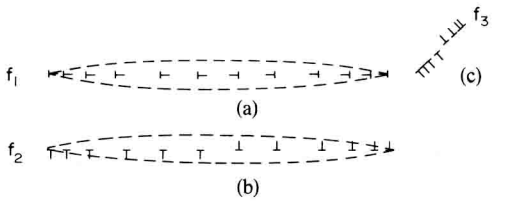

Fig. 2. Representation of the model shown in Fig. 1 in terms of continuous distributions of infinitesimal dislocations.

After resolution of the stresses σ and τ, the crack may be regarded as subjected to a stress system of σ_{y_1} normal to the crack and a shear stress of $\tau_{x_1y_1}$ and the slip band may be regarded as subjected to a stress system of a shear stress of τ_m, which are expressed respectively as follows:

$$\left.\begin{aligned} \sigma_{y_1} &= \frac{1}{2}\sigma(1-\cos 2\psi) - \tau \sin 2\psi, \\ \tau_{x_1y_1} &= \frac{1}{2}\sigma \sin 2\psi - \tau \cos 2\psi, \\ \tau_m &= -\frac{1}{2}\sigma \sin(2\theta - 2\psi) - \tau \cos(2\theta - 2\psi). \end{aligned}\right\} \tag{3}$$

And τ_i is frictional stress against dislocation movement. Equation (1) is a basic equation for the general configuration of a crack and a slip band. The stresses and the strains throughout the solid can be determined by solving eqn (1) with respect to f_1, f_2 and f_3.

2.2 *The case of the critical configuration corresponding to the low stress brittle fracture* ($\Psi = \pi/2$, $\omega = 0$ *and* $\theta = \pi/4$)

We shall now consider the relatively simple case, as a typical example[6], of the critical configuration corresponding to the low stress brittle fracture as shown in Fig. 3. The procedure of solution for the case of the general configuration in Section 2.1 is quite the same with this case in the following manner. Consider the situation where dislocations pile up against obstacles P and Q at the ends of the slip band and the number of positive dislocations and negative dislocations are equal. The model is illustrated in Fig. 3, which is equivalent to the case where $\Psi = \pi/2$, $\omega = 0$ and $\theta = \pi/4$ in Fig. 1. Equilibrium equations in this case are expressed from eqn (1) as:

$$\left.\begin{aligned} &\sigma - A\int_{-c}^{c} \frac{f_1(\zeta_1)}{\zeta_1 - x_1}\,d\zeta_1 + A\int_{-d}^{d} K_1(x_1, \zeta_2) f_3(\zeta_2)\,d\zeta_2 = 0, \\ &\tau - A\int_{-c}^{c} \frac{f_2(\zeta_1)}{\zeta_1 - x_1}\,d\zeta_1 + A\int_{-d}^{d} K_2(x_1, \zeta_2) f_3(\zeta_2)\,d\zeta_2 = 0, \\ &\tau_m - \tau_i - A\int_{-d}^{d} \frac{f_3(\zeta_2)}{\zeta_2 - x_2}\,d\zeta_2 + A\int_{-c}^{c} K_3(x_2, \zeta_1) f_1(\zeta_1)\,d\zeta_1 \\ &\qquad + A\int_{-c}^{c} K_4(x_2, \zeta_1) f_2(\zeta_1)\,d\zeta_1 = 0, \end{aligned}\right\} \tag{4}$$

where the kernels K_i ($i = 1, 2, 3, 4$) are given by the following relations from eqn (2).

$$\left.\begin{aligned} &K_1(x_1, \zeta_2) = \frac{-Y_1(Y_1^2 + X_1^2) + X_1(X_1^2 - Y_1^2)}{(X_1^2 + Y_1^2)^2}, \quad K_2(x_1, \zeta_2) = \frac{-2Y_1X_1^2}{(X_1^2 + Y_1^2)^2}, \\ &K_3(x_2, \zeta_1) = \frac{-2Y_2X_2^2}{(X_2^2 + Y_2^2)^2}, \qquad K_4(x_2, \zeta_1) = \frac{2Y_3X_3^2}{(X_3^2 + Y_3^2)^2}, \\ &X_1 = \frac{-(c - x_1) - h}{\sqrt{2}} - (d + \zeta_2), \quad Y_1 = \frac{(c - x_1) + h}{\sqrt{2}}, \quad x_2 = \frac{d + x_2}{\sqrt{2}}, \\ &Y_2 = -\frac{d + x_2}{\sqrt{2}} - (c - \zeta_1) - h, \quad X_3 = -Y_2, \qquad Y_3 = X_2. \end{aligned}\right\} \tag{5}$$

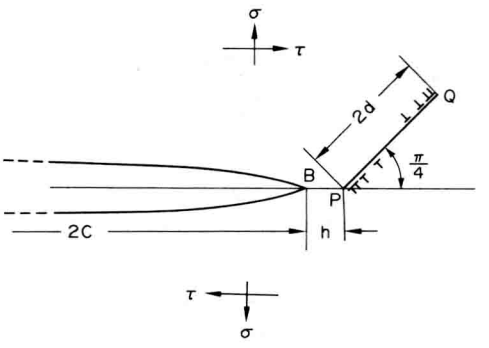

Fig. 3. A critical configuration of a crack (or a notch) and a near-by slip band.

To reduce the singular integral eqn (4), we use the condition that the continuous distribution functions $f_1(x_1)$ and $f_2(x_1)$ for the crack and $f_3(x_2)$ for the slip band are expected to be unbounded at $x_1 = \pm c$ and $x_2 = \pm d$ respectively. Under these conditions eqn (4) becomes after inversion [9]

$$\left.\begin{aligned}
f_1(x_1) &= \frac{\sigma x_1 + c_1 \pi A}{\pi A \sqrt{(c^2 - x_1^2)}} - \frac{1}{\pi^2 \sqrt{(c^2 - x_1^2)}} \int_{-c}^{c} \frac{\sqrt{(c^2 - \xi_1^2)}}{\xi_1 - x_1} \, d\xi_1 \int_{-d}^{d} K_1(\xi_1, \zeta_2) f_3(\zeta_2) \, d\zeta_2, \\
f_2(x_1) &= \frac{\tau x_1 + c_2 \pi A}{\pi A \sqrt{(c^2 - x_1^2)}} - \frac{1}{\pi^2 \sqrt{(c^2 - x_1^2)}} \int_{-c}^{c} \frac{\sqrt{(c^2 - \xi_1^2)}}{\xi_1 - x_1} \, d\xi_1 \int_{-d}^{d} K_2(\xi_1, \zeta_2) f_3(\zeta_2) \, d\zeta_2, \\
f_3(x_2) &= \frac{(\tau_m - \tau_i) x_2 + c_3 \pi A}{\pi A \sqrt{(d^2 - x_2^2)}} - \frac{1}{\pi^2 \sqrt{(d^2 - x_2^2)}} \int_{-d}^{d} \frac{\sqrt{(d^2 - \xi_2^2)}}{\xi_2 - x_2} \, d\xi_2 \int_{-c}^{c} K_3(\xi_2, \zeta_1) f_1(\zeta_1) \, d\zeta_1 \\
&\quad - \frac{1}{\pi^2 \sqrt{(d^2 - x_2^2)}} \int_{-d}^{d} \frac{\sqrt{(d^2 - \xi_2^2)}}{\xi_2 - x_2} \, d\xi_2 \int_{-c}^{c} K_4(\xi_2, \zeta_1) f_2(\zeta_1) \, d\zeta_1.
\end{aligned}\right\} \tag{6}$$

The integral constants c_1, c_2 and c_3 can be determined by the following eqns (7)–(9):

$$\int_{-c}^{c} f_1(x_1) \, dx_1 = 0, \tag{7}$$

$$\int_{-c}^{c} f_2(x_1) \, dx_1 = 0 \tag{8}$$

which are satisfied since the relative displacements of one surface of the crack to another surface are zero at the crack tip both in the x direction and in the y direction.

$$\int_{-d}^{d} f_3(x_2) \, dx_2 = 0 \tag{9}$$

which is satisfied since the number of positive dislocations and negative dislocations on the slip band are equal. Substituting eqn (6) into eqns (7)–(9), we get:

$$c_1 = c_2 = c_3 = 0. \tag{10}$$

Substituting eqn (10) into eqn (6), we can rewrite eqn (6) by changing the order of the integrations as follows:

$$\left.\begin{aligned}
f_1(x_1) &= \frac{\sigma x_1}{\pi A \sqrt{(c^2 - x_1^2)}} - \frac{1}{\pi^2 \sqrt{(c^2 - x_1^2)}} \int_{-d}^{d} L_1(x_1, \zeta_2) f_3(\zeta_2) \, d\zeta_2, \\
f_2(x_1) &= \frac{\tau x_1}{\pi A \sqrt{(c^2 - x_1^2)}} - \frac{1}{\pi^2 \sqrt{(c^2 - x_1^2)}} \int_{-d}^{d} L_2(x_1, \zeta_2) f_3(\zeta_2) \, d\zeta_2, \\
f_3(x_2) &= \frac{(\tau_m - \tau_i) x_2}{\pi A \sqrt{(d^2 - x_2^2)}} - \frac{1}{\pi^2 \sqrt{(d^2 - x_2^2)}} \int_{-d}^{d} [L_3(x_2, \zeta_1) f_1(\zeta_1) + L_4(x_2, \zeta_1) f_2(\zeta_1)] \, d\zeta_1,
\end{aligned}\right\} \tag{11}$$

where

$$\left.\begin{aligned} L_1(x_1,\zeta_2) &= \int_{-c}^{c} \frac{\sqrt{(c^2-\xi_1^2)}}{\xi_1-x_1} K_1(\xi_1,\zeta_2)\,\mathrm{d}\xi_1, \\ L_2(x_1,\zeta_2) &= \int_{-c}^{c} \frac{\sqrt{(c^2-\xi_1^2)}}{\xi_1-x_1} K_2(\xi_1,\zeta_2)\,\mathrm{d}\xi_1, \\ L_3(x_2,\zeta_1) &= \int_{-d}^{d} \frac{\sqrt{(d^2-\xi_2^2)}}{\xi_2-x_2} K_3(\xi_2,\zeta_1)\,\mathrm{d}\xi_2, \\ L_4(x_2,\zeta_1) &= \int_{-d}^{d} \frac{\sqrt{(d^2-\xi_2^2)}}{\xi_2-x_2} K_4(\xi_2,\zeta_1)\,\mathrm{d}\xi_2. \end{aligned}\right\} \tag{12}$$

The kernels $L_1(x_1,\zeta_2)$, $L_2(x_1,\zeta_2)$, $L_3(x_2,\zeta_1)$ and $L_4(x_2,\zeta_1)$ were obtained in closed forms by the complex integral on Riemann surface. The problem of determining f_1, f_2 and f_3 is reduced to the solving the simultaneous Fredholm integral equations as given by eqn (11). Since the kernels L_i ($i = 1, 2, 3, 4$) have complex form, it appears difficult to get the analytical solution, so we solved the problem numerically using a computer. Since f_1, f_2 and f_3 are expected to have singularities at the ends, we make the substitutions [6]

$$f_1(x_1) = \frac{h_1(x_1)}{\sqrt{(c^2-x_1^2)}}, \quad f_2(x_1) = \frac{h_2(x_1)}{\sqrt{(c^2-x_1^2)}}, \quad f_3(x_2) = \frac{h_3(x_2)}{\sqrt{(d^2-x_2^2)}}, \tag{13}$$

where h_1, h_2 and h_3 are differentiable in the each interval. Using eqn (13), eqn (11) can be transformed into:

$$\left.\begin{aligned} &h_1(x_1) + \frac{1}{\pi^2}\int_{-d}^{d} L_1(x_1,\zeta_2)\frac{h_3(\zeta_2)}{\sqrt{(d^2-\zeta_2^2)}}\,\mathrm{d}\zeta_2 = \frac{\sigma x_1}{\pi A}, \\ &h_2(x_1) + \frac{1}{\pi^2}\int_{-d}^{d} L_2(x_1,\zeta_2)\frac{h_3(\zeta_2)}{\sqrt{(d^2-\zeta_2^2)}}\,\mathrm{d}\zeta_2 = \frac{\tau x_1}{\pi A}, \\ &h_3(x_2) + \frac{1}{\pi^2}\int_{-c}^{c} \left[L_3(x_2,\zeta_1)\frac{h_1(\zeta_1)}{\sqrt{(c^2-\zeta_1^2)}} + L_4(x_2,\zeta_1)\frac{h_2(\zeta_1)}{\sqrt{(c^2-\zeta_1^2)}}\right]\mathrm{d}\zeta_1 = \frac{(\tau_m-\tau_i)x_2}{\pi A}. \end{aligned}\right\} \tag{14}$$

Then, let us transform the variables x_1, x_2, ζ_1, ζ_2 into ϕ, ϕ_0 as follows:

$$\left.\begin{aligned} &x_1 = c\sin\phi, \quad x_2 = d\sin\phi, \quad \left(-\frac{\pi}{2}\leqq\phi\leqq\frac{\pi}{2}\right), \\ &\zeta_1 = c\sin\phi_0, \quad \zeta_2 = d\sin\phi_0, \quad \left(-\frac{\pi}{2}\leqq\phi_0\leqq\frac{\pi}{2}\right), \end{aligned}\right\} \tag{15}$$

and introduce new functions $\bar{h}_i(\phi)$ ($i = 1, 2, 3$), $\bar{L}_i(\phi,\phi_0)$ ($i = 1, 2, 3, 4$) as follows:

$$\left.\begin{aligned} h_i(x_1) &= h_i(c\sin\phi) = \bar{h}_i(\phi), \quad (i = 1, 2), \\ h_3(x_2) &= h_3(d\sin\phi) = \bar{h}_3(\phi), \\ L_i(x_1,\zeta_2) &= L_i(c\sin\phi, d\sin\phi_0) = \bar{L}_i(\phi,\phi_0), \quad (i = 1, 2), \\ L_i(x_2,\zeta_1) &= L_i(d\sin\phi, c\sin\phi_0) = \bar{L}_i(\phi,\phi_0), \quad (i = 3, 4). \end{aligned}\right\} \tag{16}$$

Then eqn (14) can be rewritten as

$$\left.\begin{aligned} &\bar{h}_1(\phi) + \frac{1}{\pi^2}\int_{-\pi/2}^{\pi/2} \bar{L}_1(\phi,\phi_0)\bar{h}_3(\phi_0)\,\mathrm{d}\phi_0 = \frac{\sigma c}{\pi A}\sin\phi, \\ &\bar{h}_2(\phi) + \frac{1}{\pi^2}\int_{-\pi/2}^{\pi/2} \bar{L}_2(\phi,\phi_0)\bar{h}_3(\phi_0)\,\mathrm{d}\phi_0 = \frac{\tau c}{\pi A}\sin\phi, \\ &\bar{h}_3(\phi) + \frac{1}{\pi^2}\int_{-\pi/2}^{\pi/2} [\bar{L}_3(\phi,\phi_0)\bar{h}_1(\phi_0) + \bar{L}_4(\phi,\phi_0)\bar{h}_2(\phi_0)]\,\mathrm{d}\phi_0 = \frac{(\tau_m-\tau_i)d}{\pi A}\sin\phi. \end{aligned}\right\} \tag{17}$$